Experimental Determination of Electron Orbits in the Field of a Magnetic Dipole

By ERNST-ÅKE BRUNBERG, The Royal Institute of Technology, Stockholm

(Manuscript received February 18, 1952)

Abstract

An analogue method for determination of electron orbits in a magnetic dipole field has been developed by Malmfors several years ago. The method is in principle a scale model experiment in a vacuum chamber where the results are obtained by measuring the deflection of an electron beam in the field of a "terrella". During the last years this method has been further developed, and particle orbits corresponding to the following momenta have now been measured:

1) $2 \cdot 10^9 - 10^{10}\ eV/c$

Orbits arriving at magnetic latitude 58° in E, S, W and N directions at zenith angles of 0°, 20°, 40°, 60°, 80°. Orbits arriving from zenith at different latitudes beginning with 38° and continuing at intervals of 2 degrees up to the pole.

2) $10^{10} - \infty\ eV/c$

Orbits arriving at magnetic latitude

0°, 10°, 20°, 30°, 40°, 50°, 60°, 70°, 80°, and 90°

from E, S, W and N directions at zenith angles of

0°, 8°, 16°, 24°, 32°, 40°, 48°, 56°, 64°, 72°, and 80°.

The direction of orbits far away from the dipole is published as a function of momentum. The particles are assumed to move towards the earth and to be positively charged.

This article includes only diagrams for the latitudes 90°—60°. The remaining ones will be published in the next issue of this journal.

It is of great importance in cosmic physics to know the orbits of charged particles in a magnetic dipole field. This work aims to give a general survey of particle orbits in the entire range of momentum above $10^{10}\ eV/c$ and thus continues the determination of orbits in the range 10^9—$10^{10}\ eV/c$, that have been carried out earlier in the same way by MALMFORS (1945).

The problem of the paths of charged particles in a magnetic dipole field has been tackled mathematically by STÖRMER (1904—1937), LEMAITRE and VALLARTA (1936) and many others (cf. HEISENBERG, 1943, and JANOSSY, 1948) in connection with the theories of the aurora and the cosmic radiation. However, a comprehensive survey of the most important part of the energy range is still lacking.

The principle of the experiment

The method is to shoot out an electron beam from the surface of a "terrella" and then measure the deflection of the beam in the magnetic dipole field.

In this way it is possible to trace back a cosmic particle orbit and find its direction before being deflected in the earth's magnetic field.

The experiment was carried out in a cylindrical vacuum chamber made from brass, 730 mm in length with a diameter of 400 mm. The ends of the chamber were covered with thick glass plates to look through. The terrella, with electron gun, was suspended inside the chamber and 130 mm from one end. As is further explained below, the electrons could be shot out in any direction and from any latitude of the terrella. At the other end of the vacuum chamber the direction of the electron beam was measured. In this end the dipole field is practically zero, and the direction of a particle orbit here is nearly the same as at an infinite distance.

It is evident that there must exist a certain relation between the energies, dipole fields and geometric dimensions in cosmic ray case and for the model. In order to relate the model to this case the required conditions are set out below. MKSA units are used.

	Cosmic rays	Model
Radius of the earth.....	R	R_m
Magnetic dipole moment	M	M_m
Energy of particles......	V	V_m

Uniformity between the dimensions of the systems requires

$$\frac{\varrho_m}{\varrho} = \frac{R_m}{R} \qquad (1)$$

The relativistic formula for the movement of a single-charged particle in a magnetic field is:

$$B\varrho = p/e \qquad (2)$$

where $$p = \frac{1}{c}\sqrt{(eV)^2 + 2\,e\,V m_0\,c^2} \qquad (3)$$

with B = magnetic field strength
p = momentum of the particle
ϱ = radius of the curvature of the particle path
eV = particle energy
m_0 = rest mass of the particle
e = charge of the particle
c = velocity of light

It is obvious that when considering cosmic particles a relativistic treatment of their motion is necessary. For model particles, however,

$$eV \ll m_0 c^2$$

and thus equation (2) is reduced in the experiment to

$$(B\cdot\varrho)_m = 3.37\cdot 10^{-6}\cdot\sqrt{V_m} \qquad (4)$$

For the dipole field we have

$$B = \frac{\mu_0}{4\pi}\cdot\frac{M}{R^3} \qquad B_m = \frac{\mu_0}{4\pi}\cdot\frac{M_m}{R_m{}^3} \qquad (5)$$

After combining equations (1), (2), (3), (4), and (5) the following final expression is obtained with constants inserted

($R = 6.37\cdot 10^6$ m, $M = 8.11\cdot 10^{22}$ A.m^2)

$$p = 202\cdot 10^{10}\cdot\sqrt{V_m}\cdot\frac{R_m{}^2}{M_m} \qquad (6)$$

For the model we have

$R_m = 8.0\cdot 10^{-2}$ metres $\qquad V_m = 150$ volts.
$M_m = 0$—15 amp.metre^2

In the expression (6) p is in eV/c. This unit will be used in the diagrams (1—38) and if the particle energy is V electronvolts, p in these units is

$$p = V\sqrt{1 + 2\,m_0\,c^2/eV} \qquad eV/c$$

Apparatus

In the general principles the apparatus is the same as used by Malmfors (see fig. 1). The construction of the dipole and the electron gun is, however, quite different.

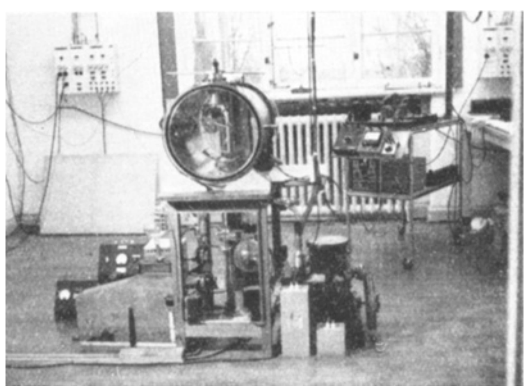

Fig. 1. View of the apparatus. The terrella can be seen in the nearest part of the vacuum chamber.

Generation of the magnetic dipole field

Malmfors used a magnet cast in *Al-Ni-Co* steel in the form of a sphere, magnetised in a homogeneous magnetic field. However, it is difficult to cast such a sphere, and irregularities in the metal will result in deviations from the exact dipole field. Measurements on the field of a cast magnet showed that the axis of the dipole was situated about 1 mm from the centre of the sphere.

The dipole field is now generated by a coil inside the hollow terrella; thereby, the above mentioned error is only 0.2 mm. The possibility of varying the strength of the magnetic field is another advantage. Eq. (6) shows that the equivalent cosmic ray momentum is a function of the magnetic dipole moment of the model, and by varying the current through the coil, the desired momentum is obtained. This could also be carried out by varying the voltage of the electron gun, but it is preferable to have a constant voltage on the gun to facilitate the focusing of the electron beam. Finally, it is a great advantage to be able to adjust the beam without the presence of the magnetic dipole field.

It can be shown (HARNWELL, 1938) that a spherical coil generates a magnetic dipole field when wound in such a manner that the current density along an arc in the meridian plane is proportional to the sine of the polar distance.

A solid coil could be built up of many concentric spheres and a magnetic dipole M obtained by superposition. It is easier, however, to use a number of coaxial cylindrical coils and a suitable design has been given by BROWN and SWEER (1945).

Fig. 2 shows a crossection of the construction. Insulated copper wire (a) was wound on a brass core (b). The layers were separated from each other with paper and bakelite varnish. The whole coil was enclosed in a copper shell (c) and baked at a temperature of + 120 °C. Afterwards, the copper shell was evacuated to a pressure of 1 μ. The evacuation was necessary to prevent possible bursting of the shell when placed in a vacuum chamber. The diameter of the wire was 0.6 mm and the entire resistance 50 Ω.

The measurements of the generated magnetic field were carried out by means of a rotating fluxmeter coil of sufficiently small dimensions. The induced voltage was measured with a vacuum tube voltmeter. The variation of the field along the arc from pole to pole was compared with an ideal dipole field; the deviation was smaller than the probable average error of measurements (about 2 %). The same range of deviation was obtained when measuring the field along a radius and comparing it with the r^{-3}-curve.

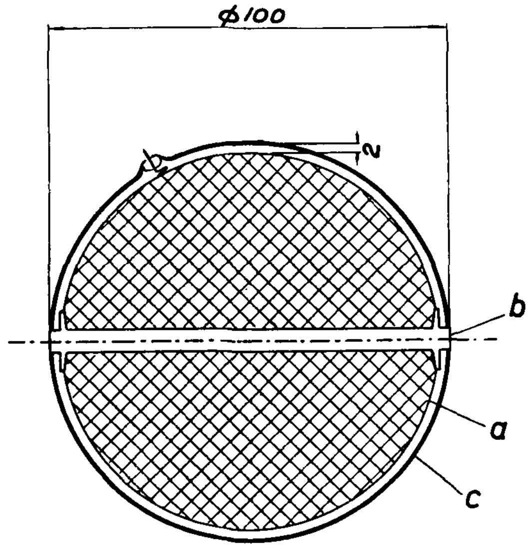

Fig. 2. Construction of the terrella. (Dimensions in millimeters.)

The dipole was calculated to

$$M = 10.73 \text{ amp.m}^2/\text{amp. magnetizing current.} \tag{7}$$

It was necessary to compensate the earth's magnetic and other disturbing fields. Good compensation was achieved by placing current coils on the walls, ceiling and floor of the room. The magnetic field thus left in the vacuum chamber was less than 0.03 gauss.

Instruments were placed at a safe distance from the vacuum chamber or were magnetically screened.

The electron gun

The electron gun required an electrode system with small dimensions to give a well defined electron beam with a diameter of 1—2 cm after more than half a metre travel.

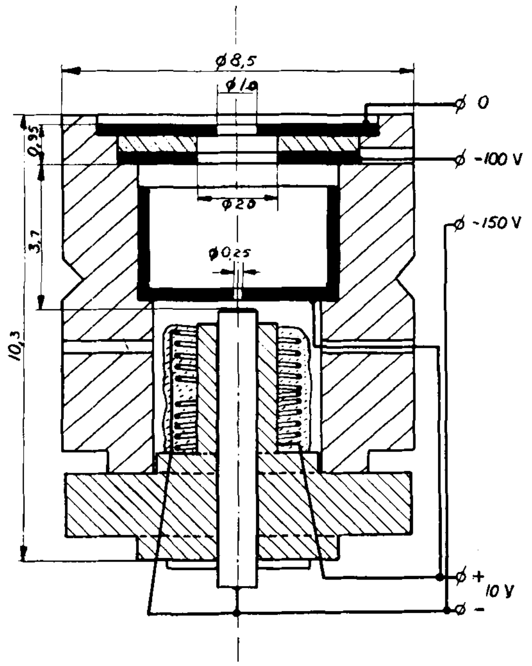

Fig. 3. Construction of the electron gun. (Dimensions in millimeters.)

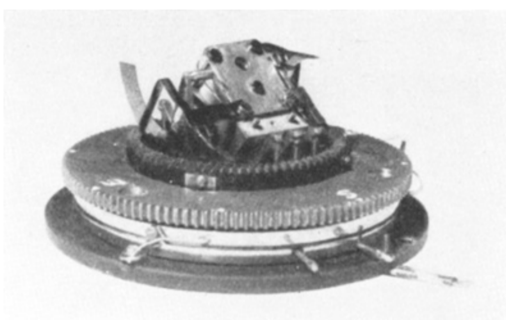

Fig. 4. The electron gun in its mounting.

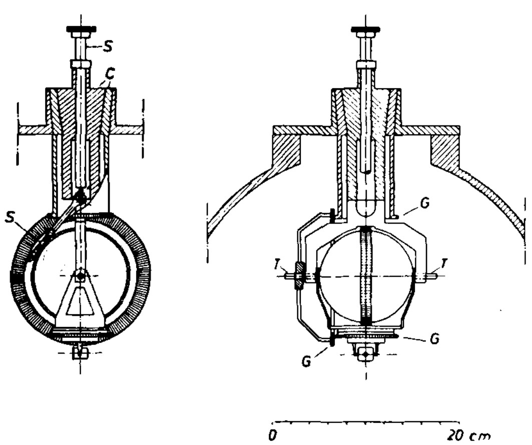

This short electrode system was necessary, otherwise the electrons would be appreciably deflected by the magnetic field before leaving the gun and lead to an error in the direction in which the electrons are shot out. The gun meets the specified requirements except in some few directions, perpendicular or nearly perpendicular to the magnetic lines of force. Especially in the lower momentum range, this deviation can be noticeable as discussed more in detail in the next section.

The experiment was carried out in a vacuum of 10^{-5} mm Hg.

Fig. 3 shows a drawing of the electron gun. The body is made of ceramic material ("Pyrophyllite") which can be machined, but hardens after firing. The electrode system is made of molybdenum plates. The cathode is a nickel wire with a diameter of 1 mm coated on the end surface. It can easily be replaced when the emission has been reduced through poisoning or other destruction of the carbonate film. The cathode is indirectly heated by a tungsten spiral, the last turns of which are reversed to avoid any disturbing magnetic field inside the electrode system. Fig. 4 gives a picture of the gun in its mounting.

Fig. 5 is a diagram showing the principle of fixing the terrella and electron gun in the vacuum chamber. By means of the screw (*S*), the model earth with mounting and gun can be moved around the trunnions *T—T*. The gun in its mounting can be turned in the horizontal plane with respect to the terrella by means of vacuum-tight cones (*C*) and gears (*G*). For each turn the gun is moved through 8° in zenith angle by means of a cross and bevel gear drive (see fig. 6).

Finally it is possible, from outside the vacuum chamber, to alter the latitude of the gun on the model by means of a friction drive between the model and the gun mounting. This arrangement is not shown on the figure.

Determination of direction

Fig. 7 shows the method for determining the direction of the electron beam as used by Malmfors. For a given energy and direction of emis-

Fig. 5. Construction of the system carrying the terrella and the electron gun.

sion, a certain path is obtained. The model (with gun) is turned until the beam strikes a plate with specially shaped teeth. The shadow of some tooth can be seen in the spot on the fluorescent screen. The quantities m, n and l give then the direction of the electron beam at a long distance from the dipole. The difference between its direction here and at an infinite distance due to the deflection in the fringe of the dipole field is only one or two degrees, and is determined by an approximate method worked out by Malmfors (cf. page 24).

The results of measurements are given in the form of two angles (see fig. 8) Φ_N, the north latitude angle and Ψ_E, a longitude angle, reckoned eastwards from the meridional plane through the electron gun. These angles cannot be directly read in the measurements but are calculated from the measured direction on the screen.

The error in the initial direction of the electrons, which is due to the deflection of the electron beam inside the electron gun, has been estimated in the following manner.

According to Malmfors, the deflection can be approximately determined from

$$\omega_0 = \frac{2\, a_0 \cdot B}{3.37 \cdot 10^{-6}\,\sqrt{V_m}} \cdot \sin\gamma \tag{8}$$

where B = magnetic field strength

$3.37 \cdot 10^{-6}\,\sqrt{V_m} = B \cdot \varrho$

a_0 = distance between the cathode and the anode

V_m = acceleration voltage

γ = the angle between the electron gun and the magnetic field.

It is assumed that B is a constant inside the electrode system, and that the electric field strength is constant along the axis of the system between the cathode and the anode.

As $a_0 = 0.46$ cm and $V_m = 150$ volts we obtain in degrees $\omega_0{}^0 = 0.13 \cdot B \sin\gamma$.

In the present electrode system, however, the electric field is weaker in the vicinity of the cathode and then increases towards the anode. Thus the error ought to be greater than stated above.

A graphic determination of the error inside the electrode system sustained these assumptions. The error was estimated to be

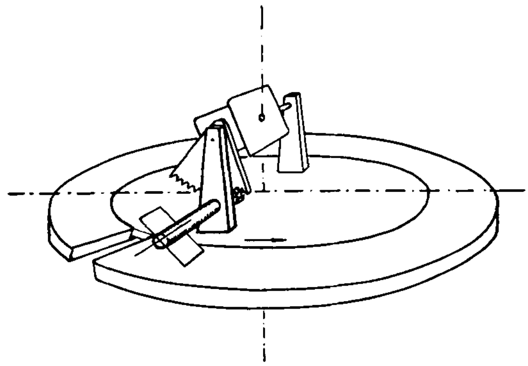

Fig. 6. Method for adjusting the zenith- and azimuth angles of the gun.

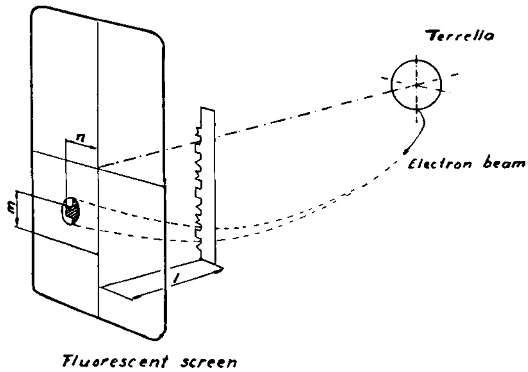

Fig. 7. Determination of the direction of the beam.

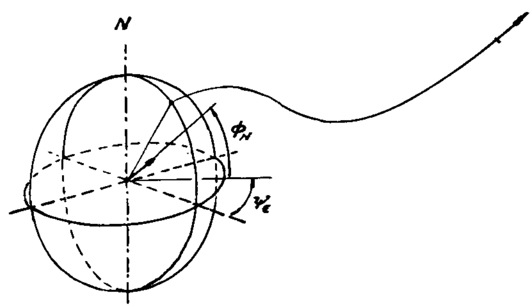

Fig. 8. The angles of Ψ_E and Φ_N in the system of coordinates of the terrella.

$$\omega^0 = 1.3 \cdot \omega_0{}^0 \tag{9}$$

When the initial direction of the electrons lies in the E—W plane at latitude $\lambda = 0°$, the error means that the direction is more easterly than is given from the geometric direction of the gun. The correction amounted to 10°—15° in the lowest energy range.

As a control the curves have been compared with values calculated by Störmer (cf. *Astrophysica Norvegica*, Vol. II No. 1). These orbits are given in the following table together with corresponding values corrected for deflection inside the gun.

Störmer orbit No.	eV/c	Zenith angle	(Störmer) Ψ	Ψ_E
70	$2.23 \cdot 10^{10}$	16°	71°	72°
68	$3.03 \cdot 10^{10}$	38°	24°	24°
69	»	15°	46°	46°
71	»	27°	106°	109°
71	$2.23 \cdot 10^{10}$	8°	109°	107°

The difference between the measured values Ψ_E and the very accurate calculations by Störmer does not exceed 3° which is satisfactory.

In order to compensate the deflection inside the electron gun the axis of the gun has been tilted so much that the electrons leave the gun in the desired direction.

When it was impossible to adjust the zenith angle because of the construction of the gun's mounting (only angles of 8°, 16°, 24°... were possible) two zenith angles were measured and the intermediate value interpolated. The values thus obtained correspond to the directions (N, S, E or W) in the diagrams.

Calculation of Φ_N and Ψ_E

The angles Φ_N and Ψ_E are obtained from the measured distances m, n and l on the screen and the angles v and A (fig. 9) using the following trigonometric relations:

$$\left.\begin{aligned}
S_{OL} &= l \sin v + n \cos v \\
S_{OM} &= (l \cos v - n \sin v) \sin A - m \cos A \\
S_{ON} &= -(l \cos v - n \sin v) \cos A - m \sin A \\
\operatorname{tg} \Phi_N &= \frac{S_{ON}}{\sqrt{S_{OL}^2 + S_{OM}^2}} \quad \operatorname{tg} \Psi_E = \frac{S_{OL}}{S_{OM}}
\end{aligned}\right\} \quad (10)$$

The first 3 formulae show the transition from the system of coordinates at the screen to the system (OL, OM, ON) at the terrella.

Over the whole range of energies 10,000 points of measurements were required. In these circumstances even the calculations by equations (10) would take a long time and a simple calculating machine was built to reduce

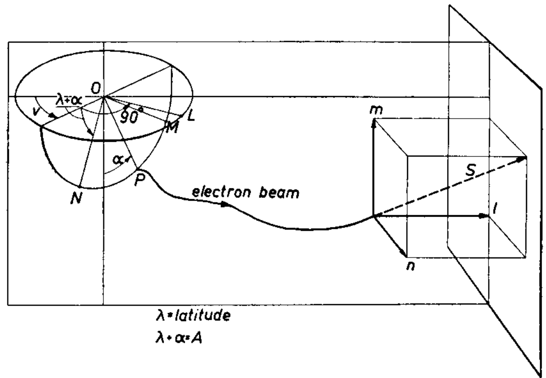

Fig. 9. Sketch showing the calculation of the final direction of the orbits.

the work. The time for calculation of S_{OM} and S_{ON}, namely about 6 minutes manually, was reduced to about 1.5 minutes. The measurement and complete calculation required about 6 minutes for each point.

Fig. 10 shows the principle used for the calculating machine. The accuracy of the machine was approximately 0.5 %.

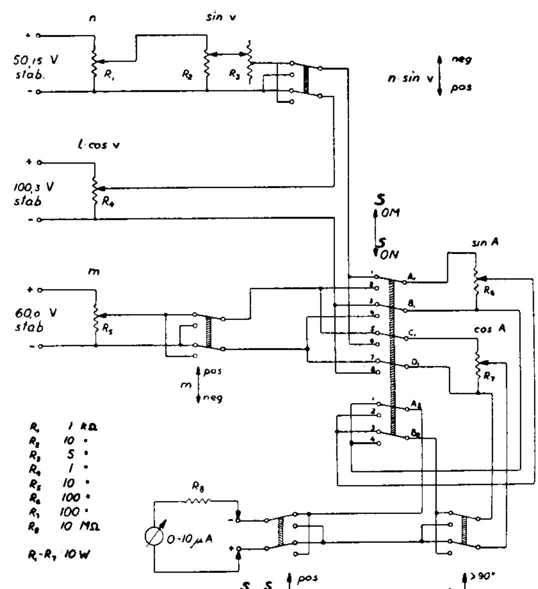

Fig. 10. The principle of the calculating machine. The following expressions can be solved:

$$S_{OM} = (l \cdot \cos v - n \cdot \sin v) \cdot \sin A - m \cos A$$
$$S_{ON} = (l \cos v - n \cdot \sin v) \cdot \cos A - m \sin A$$

Measurements

Measurements have been taken for each 10° of latitude beginning at the equator. Φ_N and Ψ_E have been drawn for each latitude and for paths starting in North, South, East and West directions as a function of momentum. Each latitude is represented by four diagrams:

Ψ_E in the N—S plane
Φ_N in the N—S »
Ψ_E in the E—W »
Φ_N in the E—W »

In the diagram the dot-dashed curve marked 0° corresponds to particles which arrive from zenith; curves marked 8° N, 16° N, 24° N, etc. correspond to particles arriving from north and make angles of 8°, 16°, 24°, etc. with the zenith. Curves marked 8° S, 16° S, 24° S, etc. correspond to particles arriving in the same way from South.

The diagrams give the direction of the path at an infinite distance from the dipole as a function of momentum. The particles arriving at the earth are positively charged.

Accuracy of measurements

The results of the experiment are to be applied to research on cosmic rays in the magnetic field of the earth. The obtained average error in the experiment did not exceed 2—3°. Experimental errors of this magnitude, however, can be neglected, because of the considerable deviation of the terrestrial magnetic field from a dipole field.

Accuracy in determination of the angles Ψ_E and Φ_N depends mostly on errors in reading of m, n and ν. According to equation (10) we have

$$(\delta\Phi)^2 + \cos^2\Phi \cdot (\delta\psi)^2 = \left(\frac{\delta m}{l}\right)^2 + \left(\frac{\delta n}{l}\right)^2 + (\delta\nu)^2 \qquad (11)$$

If $l = 100$ mm, $m = 2$ mm, $n = 2$ mm, $\nu = 2°$ we get

$$\sqrt{(\delta\Phi)^2 + \cos^2\Phi\cdot(\delta\Psi)^2} = 3°.5$$

in the greater majority of cases. This gives an average error in Φ and Ψ of 2—3°.

It should be pointed out that, according to equation (11), the uncertainty rises rapidly when $\Phi \to 90°$. This is not a real error but depends only on the chosen system of coordinates. In these special cases the velocity vector is projected on a plane nearly perpendicular to itself; therefore, it is difficult to determine Ψ_E. An approximate calculation shows, however, that even when Φ_N reaches values of 70—75°, the error still does not exceed 3°. Curves where the error is expected to exceed 3° are dashed. As can be seen from the diagrams, this happens when Φ_N is near 90°.

For accuracy in determination of momentum p we have the following expression

$$\left|\frac{\Delta p}{p}\right| = \left|\frac{1}{2}\cdot\frac{\Delta V_m}{V_m}\right| + \left|2\cdot\frac{\Delta R_m}{R_m}\right| + \left|\frac{\Delta M_m}{M_m}\right|$$

derived from equation (6).

If $\frac{\Delta V_m}{V_m} = 1\%$ $\frac{\Delta M_m}{M_m} = 2.5\%$ $\frac{\Delta R_m}{R_m} = 1.3\%$

we obtain $\frac{\Delta p}{p} \approx 5.5\%$

The investigation of systematic errors was carried out by comparing measurements at one place in the northern hemisphere, it's antipodal point in the southern hemisphere and two more points symmetrical to the equatorial plane. Deviation of these values was supposed to show eventual asymmetry of the apparatus, influence of extraneous magnetic fields, etc. These deviations were also $< 3°$.

Besides these investigations, a control of the accuracy was made by comparison of the results with values calculated by STÖRMER (cf. *Astrophysica Norvegica*, Vol. II No. 1). The accuracy of his calculations was stated to be

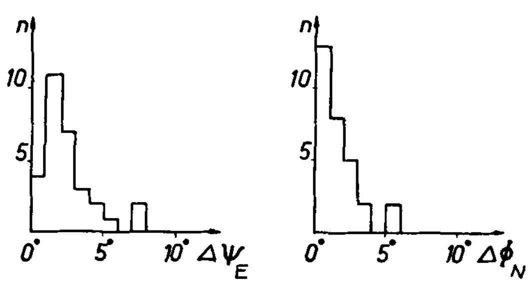

Fig. 11. Random distribution of Ψ_E and Φ_N.

about 0.2°. About 30 values were chosen from this work and special measurements were made with the apparatus. The x-axis in the diagrams of fig. 11 represents the angle error in degrees, and the y-axis the number of observations. The diagrams show that the average angle error is 2—2.5°, in rather good agreement with the expected range of error.

In addition to this some Störmer orbits have been compared with values found by interpolation in the diagrams (1—38).

The result is shown below. In most cases it was necessary to interpolate these values from several curves and diagrams; therefore, it is natural if the error is somewhat greater than found above.

No.	Momentum	λ	Zenith angle	Ψ (Störmer)	Φ (Störmer)	Ψ_E	Φ_N
9	$1.59 \cdot 10^{11}$	52°	52°	1°	0	—2°	—1°
1	,,	76°	79°	—19°	0	—22°	2°
63	,,	0	33°	—21°	0	—20°	0
19	$6.21 \cdot 10^{10}$	66°	63°	38°	0	30°	5°
64	,,	0	90°	—45°	0	—43°	0
19	$5.01 \cdot 10^{10}$	65°	70°	70°	0	64°	3°
65	,,	0	73°	—27°	0	—27°	0
66	$3.96 \cdot 10^{10}$	0	70°	—13°	0	—14°	—1°
31	..	51°	39°	36°	0	32°	—4°
43	$1.55 \cdot 10^{10}$	57°	40°	31°	0	31°	2°

The threshold values of the forbidden cones could not be exactly determind because of the small dimensions of the apparatus. However, the curves indicate a tendency toward the values calculated by LEMAITRE and VALLARTA for 0°, 20° and 30° latitude (cf. *Phys. Rev.* 1936, Vol. 50., p. 500).

Acknowledgments

I want to express my sincere thanks to Mr A. Dattner for his help with the experiment, especially the measurements.

I also want to thank Dr K.-G. Malmfors and Dr N. Herlofson for many discussions and valuable advice.

Professor C. Störmer very kindly placed his original calculations at my disposal, for which I am very grateful.

Finally it is a pleasure for me to thank Mr H. Ekstrand for building some parts of the apparatus and Mr H. Witt for his computing work.

The investigation has been made financially possible by grants from Statens Naturvetenskapliga Forskningsråd.

REFERENCES:

BROWN, JR. W., and J. H., SWEER, 1945: "The Fluxball", *Ref. of Sc. Instr.* **16**, No. 10. p. 276.

HARNWELL, G. P., 1938: *Principles of Electricity and Magnetism*, Mc. Graw-Hill Book Co. Inc. p. 376.

HEISENBERG, W., 1943: *Kosmische Strahlung*, Berlin, Springer-Verlag.

JÁNOSSY, L., 1948: *Cosmic Rays*, Oxford.

JOHNSSON, T. H., 1938: Rev. of Mod. Phys. **10**, p. 193.

LEMAÎTRE, G., and M. S. VALLARTA, 1936, a: "On the Geomagnetic Analysis of Cosmic Radiation", *Phys. Rev.* **49**, p. 719.

LEMAÎTRE, G., and, M. S. VALLARTA, 1936, b: "On the Allowed Cone of Cosmic Radiation", *Phys. Rev.* **50**, p. 493.

MALMFORS, K. G., 1945: "Determination of Orbits in the Field of a Magnetic Dipole with Applications to the Theory of the Diurnal Variation of Cosmic Radiation" *Arkiv för Matematik, Astronomi och Fysik* 32 A, No 8.

STÖRMER, C., 1904: Sur le mouvement d'un point materiel portant une charge d'électricité sous l'action d'un aimant élémentaire". *Videnskabs-selskabet i Christiania.*

STÖRMER, C., 1934—1937: "On the Trajectories of Electric Particles in the Field of a Magnetic Dipole with Applications to the Theory of Cosmic Radiation". *Astrophysica Norvegica*, Oslo. Vol. I No. 1, June 1034, Vol. 1 No. 4, April 1935; Vol. II No. 1, June 1936; Vol. II No 4,J an. 1937.

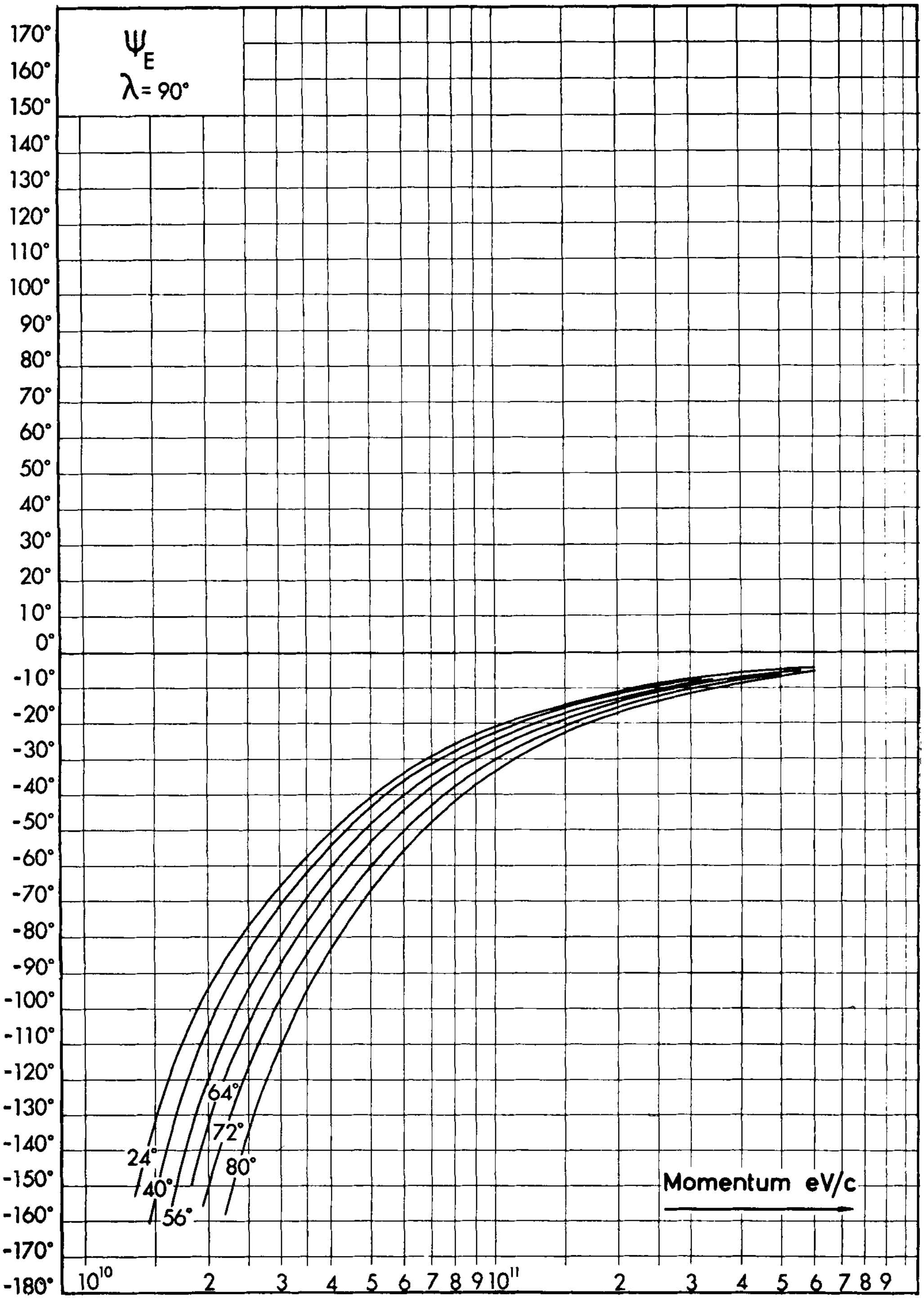

ψ_E
$\lambda = 90°$
170°
160°
150°
140°
130°
120°
110°
100°
90°
80°
70°
60°
50°
40°
30°
20°
10°
0°
-10°
-20°
-30°
-40°
-50°
-60°
-70°
-80°
-90°
-100°
-110°
-120°
-130°
-140°
-150°
-160°
-170°
-180°
24°
40°
56°
64°
72°
80°
Momentum eV/c
10^{10} 2 3 4 5 6 7 8 9 10^{11} 2 3 4 5 6 7 8 9

Diagram 1

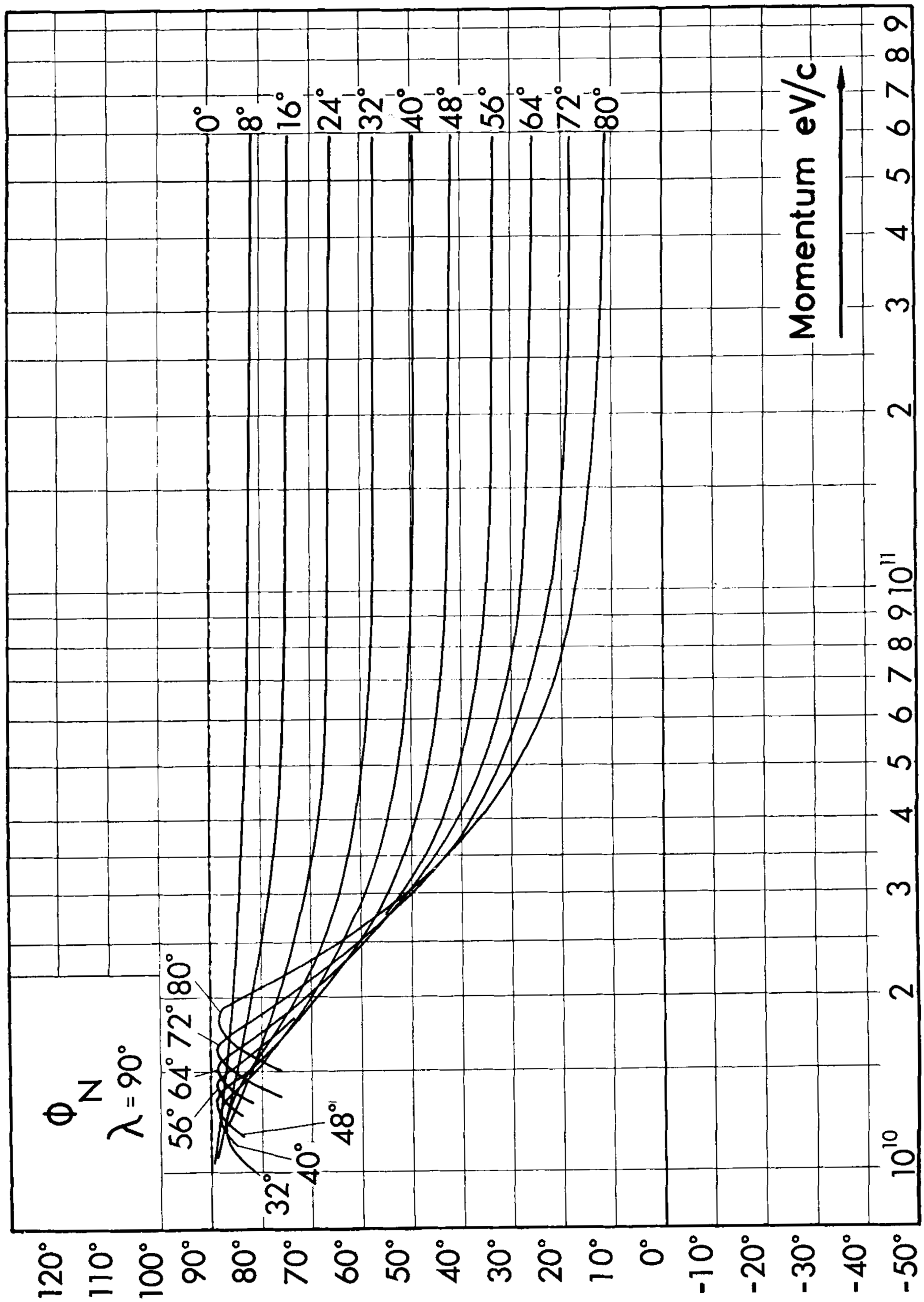

Φ_N
$\lambda = 90°$
Momentum eV/c
0° 8° 16° 24° 32° 40° 48° 56° 64° 72° 80°
56° 64° 72° 80°
32° 40° 48°
10^{10} 2 3 4 5 6 7 8 9 10^{11} 2 3 4 5 6 7 8 9
120° 110° 100° 90° 80° 70° 60° 50° 40° 30° 20° 10° 0° -10° -20° -30° -40° -50°

Diagram 2

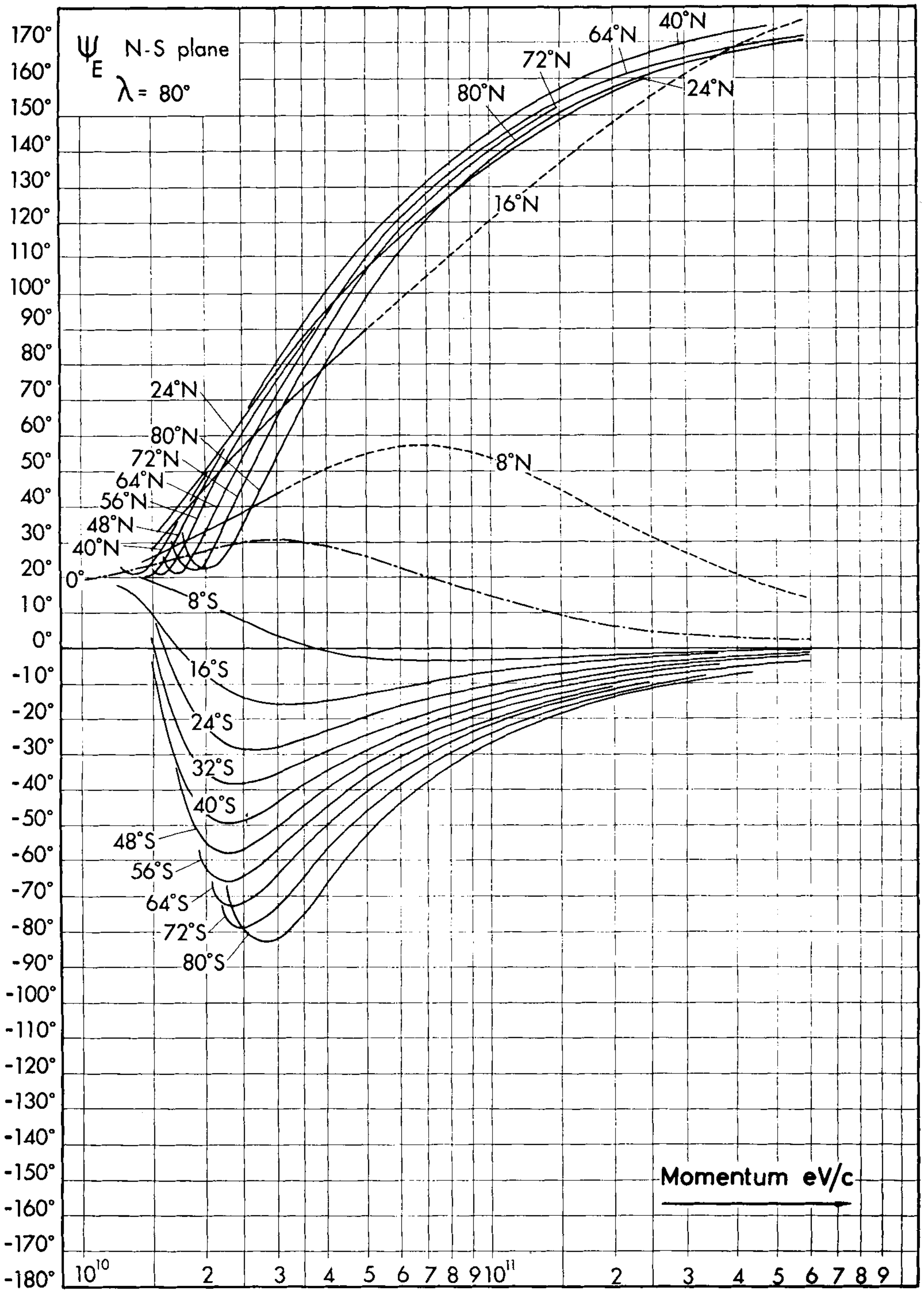

ψ_E N-S plane
λ = 80°
170°
160°
150°
140°
130°
120°
110°
100°
90°
80°
70°
60°
50°
40°
30°
20°
10°
0°
-10°
-20°
-30°
-40°
-50°
-60°
-70°
-80°
-90°
-100°
-110°
-120°
-130°
-140°
-150°
-160°
-170°
-180°
40°N
64°N
72°N
80°N
24°N
16°N
24°N
80°N
72°N
64°N
56°N
48°N
40°N
0°
8°N
8°S
16°S
24°S
32°S
40°S
48°S
56°S
64°S
72°S
80°S
Momentum eV/c
10^{10} 2 3 4 5 6 7 8 9 10^{11} 2 3 4 5 6 7 8 9

Diagram 3

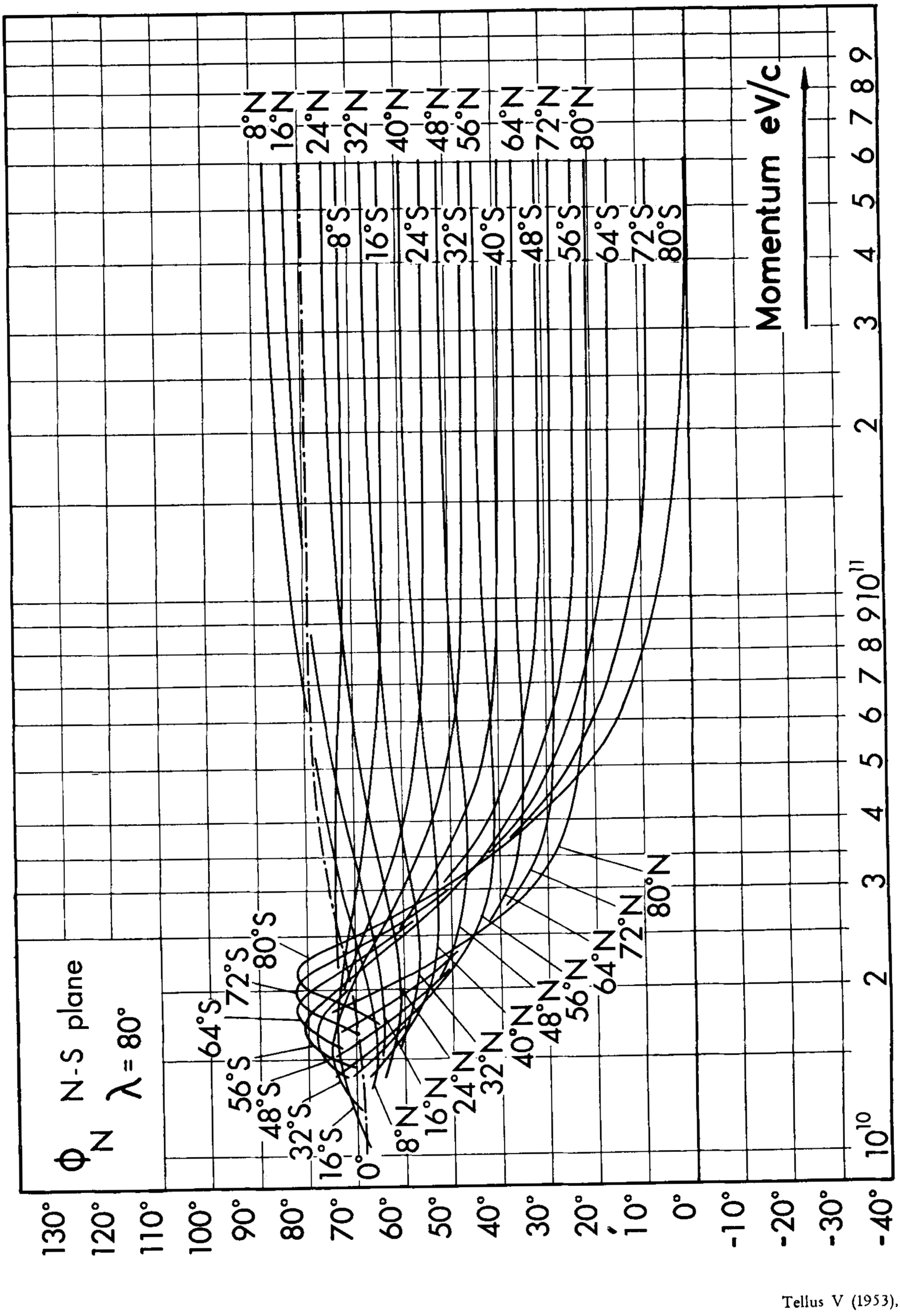

Diagram 4

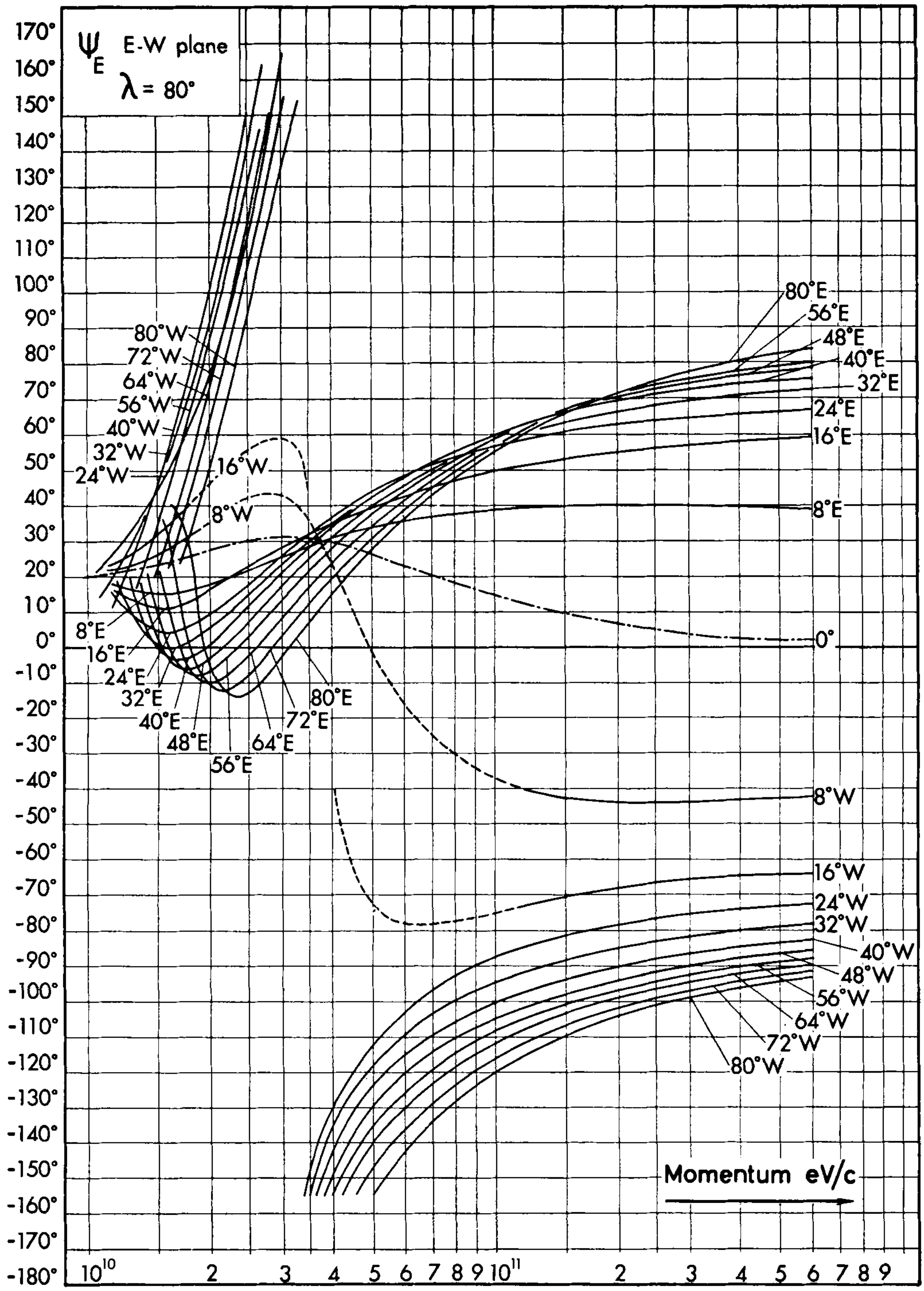

ψ_E E-W plane
$\lambda = 80°$
Momentum eV/c
80°E
56°E
48°E
40°E
32°E
24°E
16°E
8°E
0°
8°W
16°W
24°W
32°W
40°W
48°W
56°W
64°W
72°W
80°W

Diagram 5.

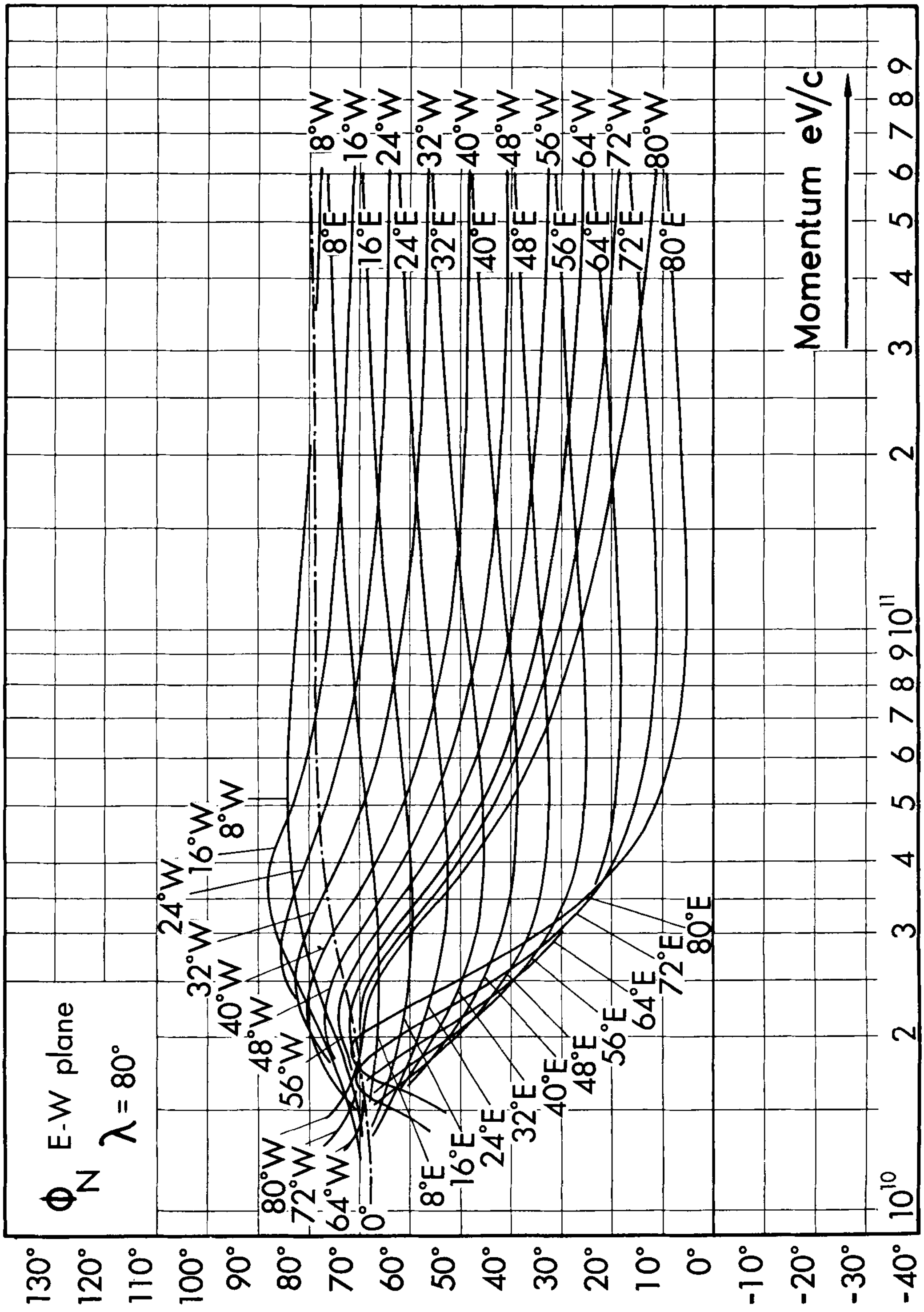

Φ N E-W plane
λ = 80°
Momentum eV/c
10^10 2 3 4 5 6 7 8 9 10^11 2 3 4 5 6 7 8 9
130° 120° 110° 100° 90° 80° 70° 60° 50° 40° 30° 20° 10° 0° -10° -20° -30° -40°
8°W 16°W 24°W 32°W 40°W 48°W 56°W 64°W 72°W 80°W
8°E 16°E 24°E 32°E 40°E 48°E 56°E 64°E 72°E 80°E
0°

Diagram 6.

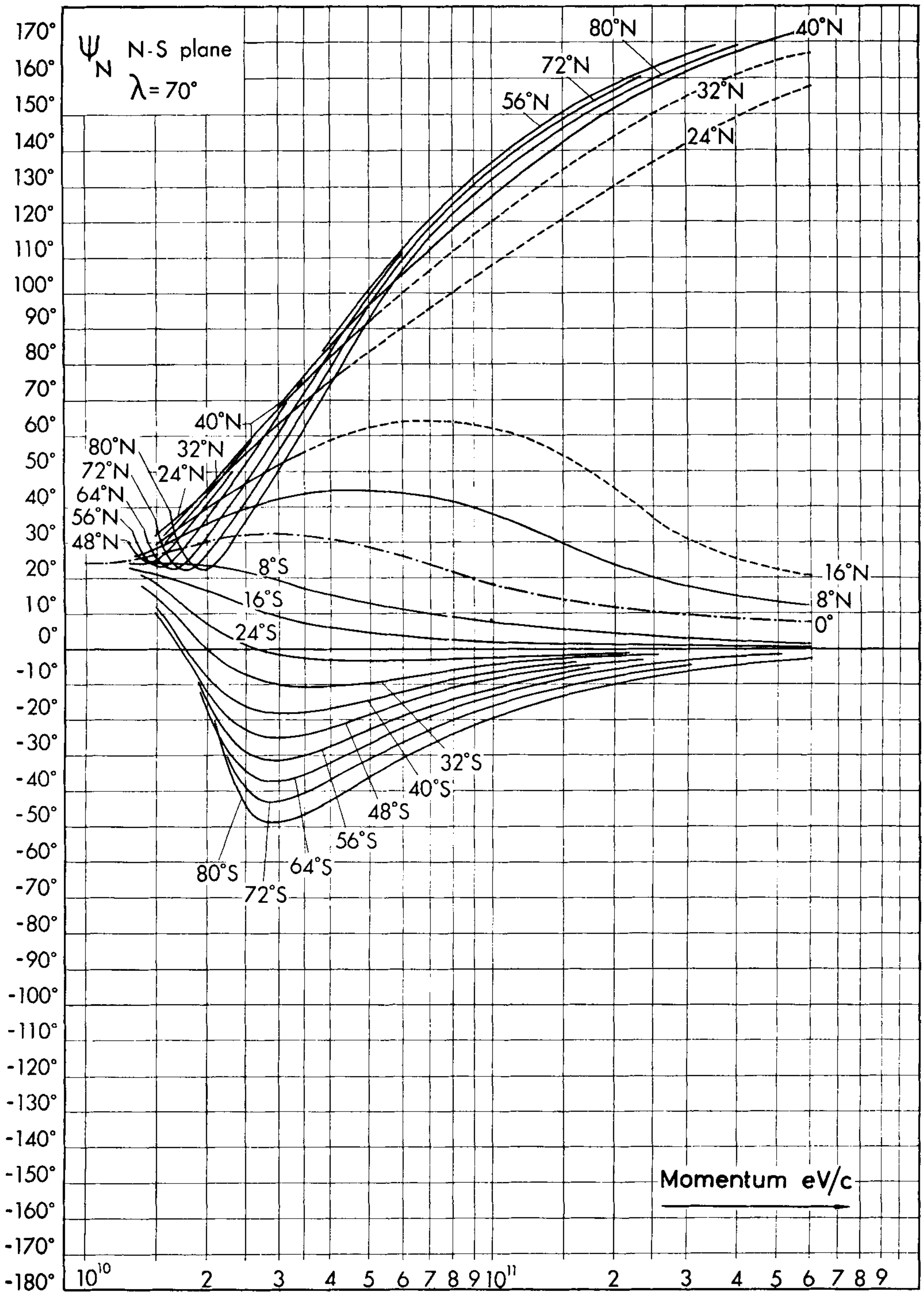

ψ_N N-S plane
$\lambda = 70°$
170°
160°
150°
140°
130°
120°
110°
100°
90°
80°
70°
60°
50°
40°
30°
20°
10°
0°
-10°
-20°
-30°
-40°
-50°
-60°
-70°
-80°
-90°
-100°
-110°
-120°
-130°
-140°
-150°
-160°
-170°
-180°
80°N
72°N
56°N
40°N
32°N
24°N
40°N
80°N
32°N
72°N
24°N
64°N
56°N
48°N
8°S
16°S
24°S
16°N
8°N
0°
32°S
40°S
48°S
56°S
64°S
80°S
72°S
Momentum eV/c
10^{10}
2
3
4
5
6
7
8
9
10^{11}
2
3
4
5
6
7
8
9

Diagram 7.

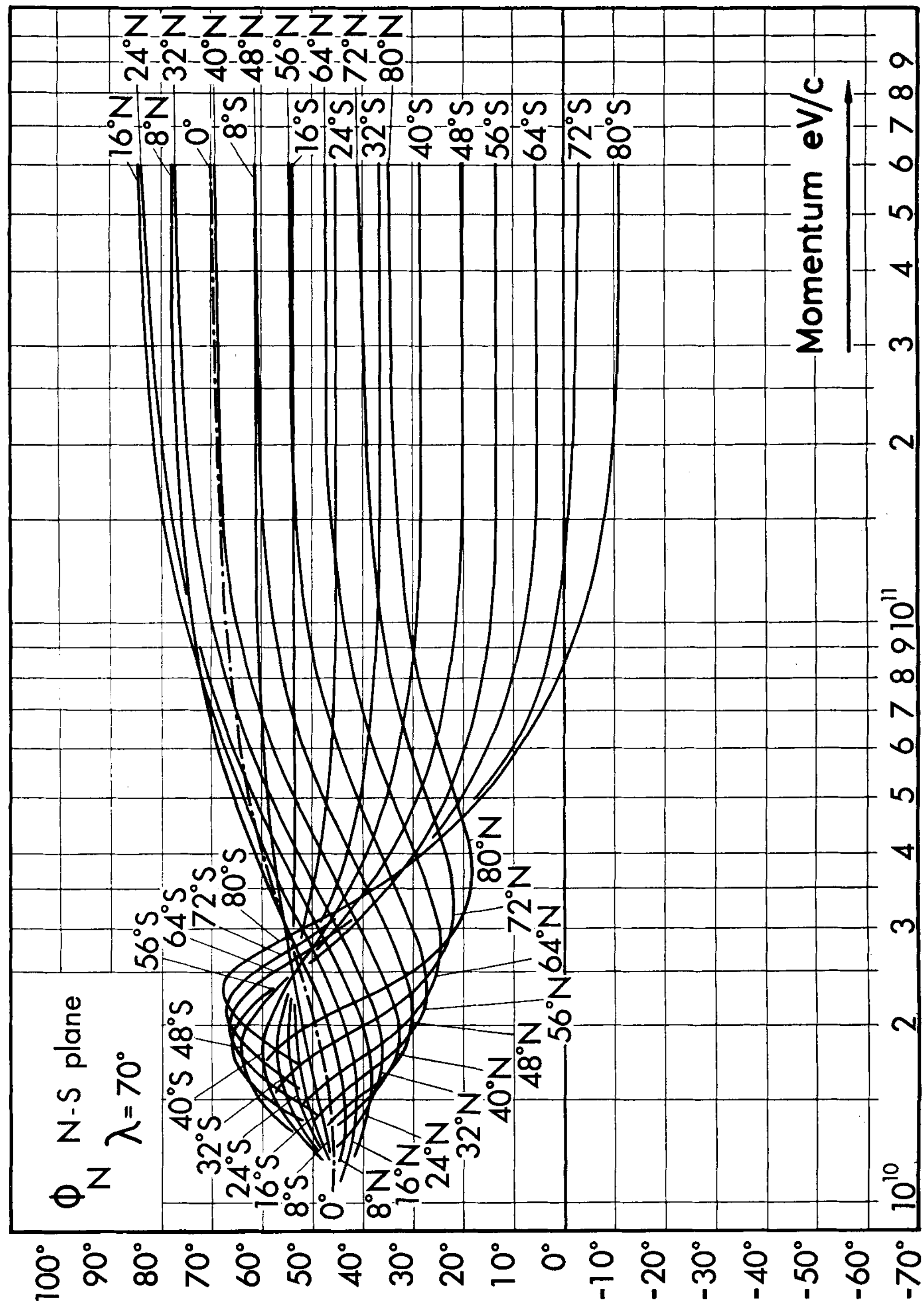

Φ_N N-S plane
$\lambda = 70°$
Momentum eV/c
10^{10}
10^{11}
100° 90° 80° 70° 60° 50° 40° 30° 20° 10° 0° -10° -20° -30° -40° -50° -60° -70°

Diagram 8.

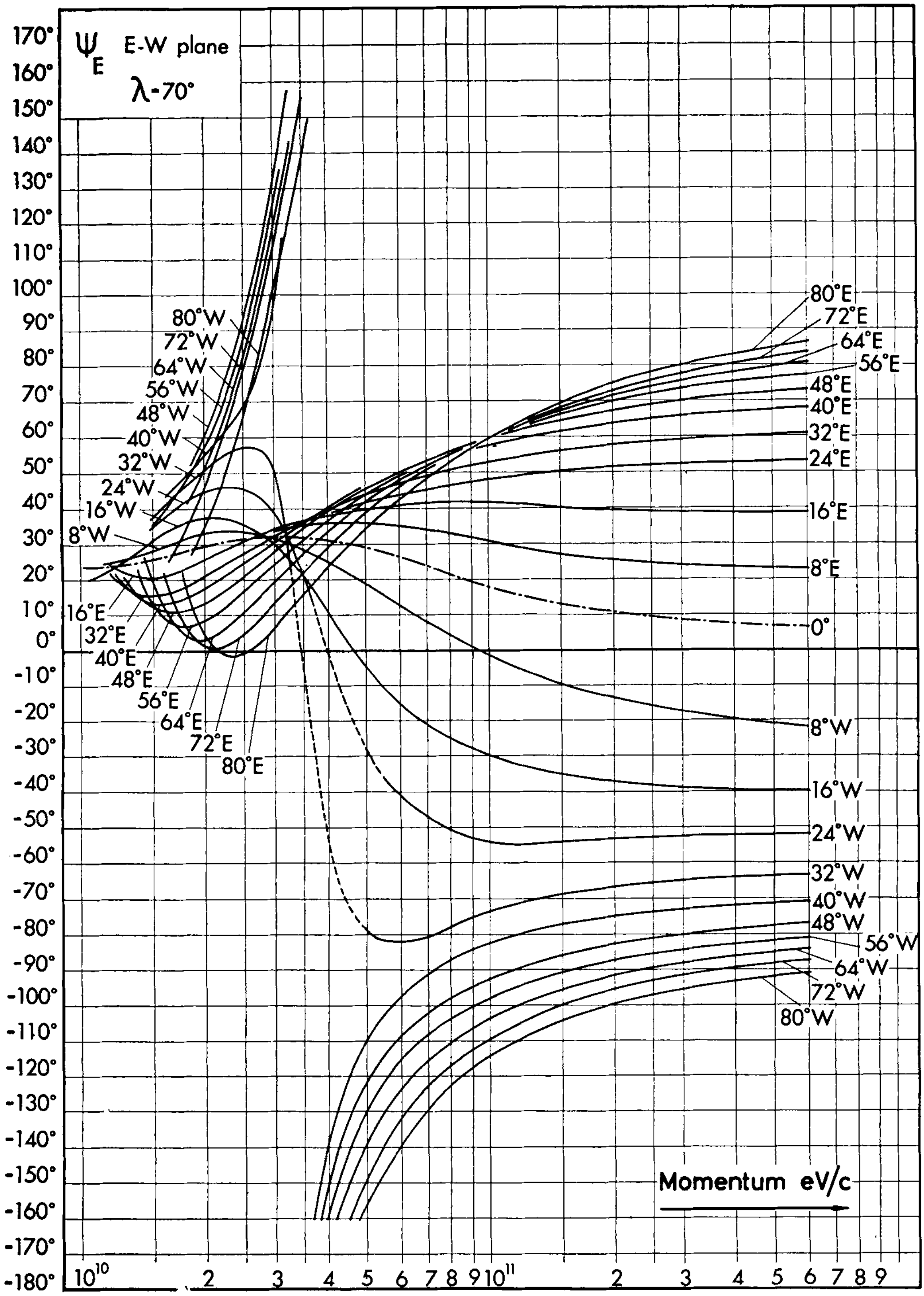

ψ_E E-W plane
λ-70°
170°
160°
150°
140°
130°
120°
110°
100°
90°
80°
70°
60°
50°
40°
30°
20°
10°
0°
-10°
-20°
-30°
-40°
-50°
-60°
-70°
-80°
-90°
-100°
-110°
-120°
-130°
-140°
-150°
-160°
-170°
-180°
80°W
72°W
64°W
56°W
48°W
40°W
32°W
24°W
16°W
8°W
16°E
32°E
40°E
48°E
56°E
64°E
72°E
80°E
80°E
72°E
64°E
56°E
48°E
40°E
32°E
24°E
16°E
8°E
0°
8°W
16°W
24°W
32°W
40°W
48°W
56°W
64°W
72°W
80°W
Momentum eV/c
10^{10}
2
3
4
5
6
7
8
9
10^{11}
2
3
4
5
6
7
8
9

Diagram 9.

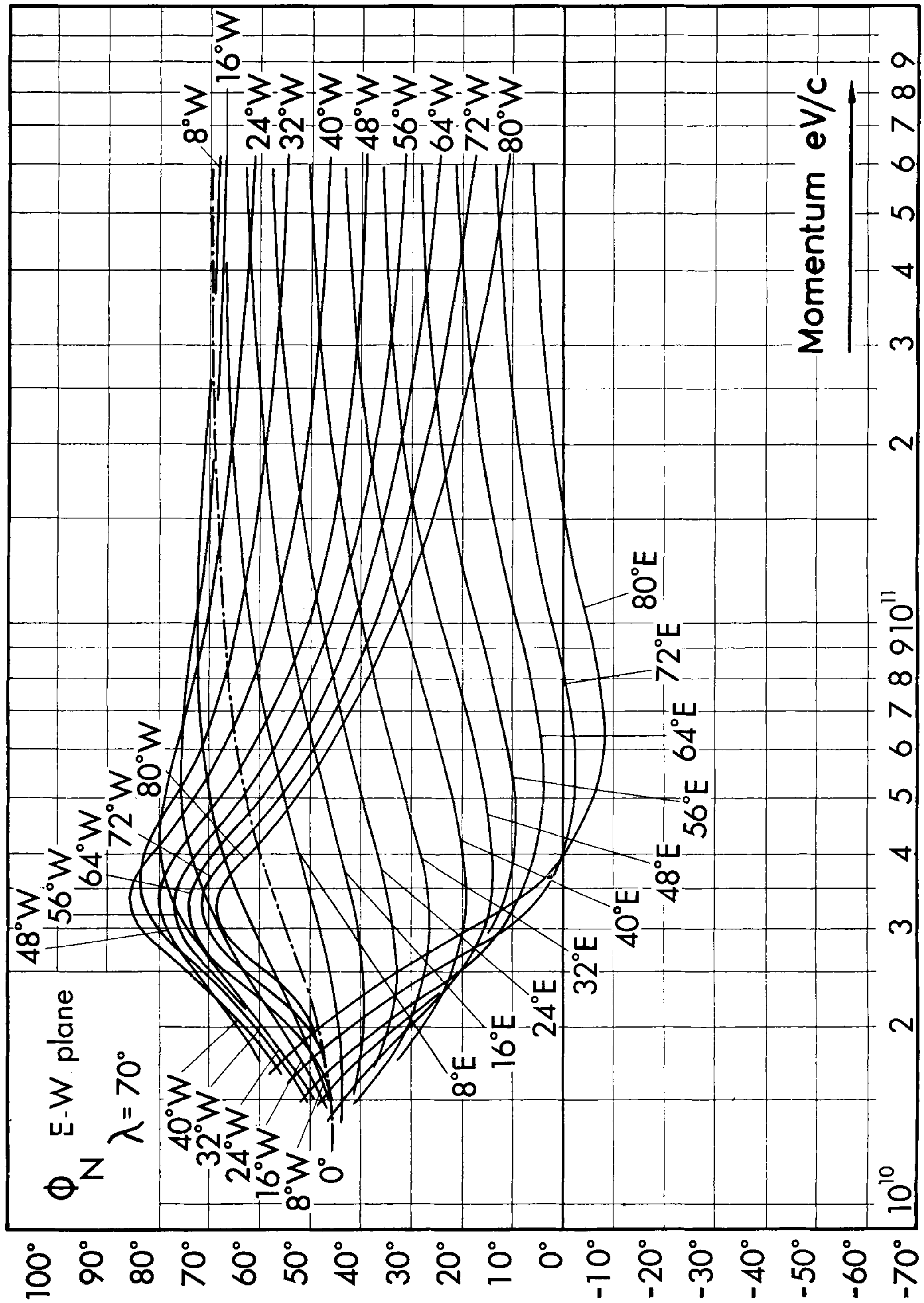

Φ N E-W plane
λ = 70°
Momentum eV/c
10^10
2
3
4
5
6
7
8
9
10^11
100°
90°
80°
70°
60°
50°
40°
30°
20°
10°
0°
-10°
-20°
-30°
-40°
-50°
-60°
-70°
8°W
16°W
24°W
32°W
40°W
48°W
56°W
64°W
72°W
80°W
0°
8°E
16°E
24°E
32°E
40°E
48°E
56°E
64°E
72°E
80°E

Diagram 10.

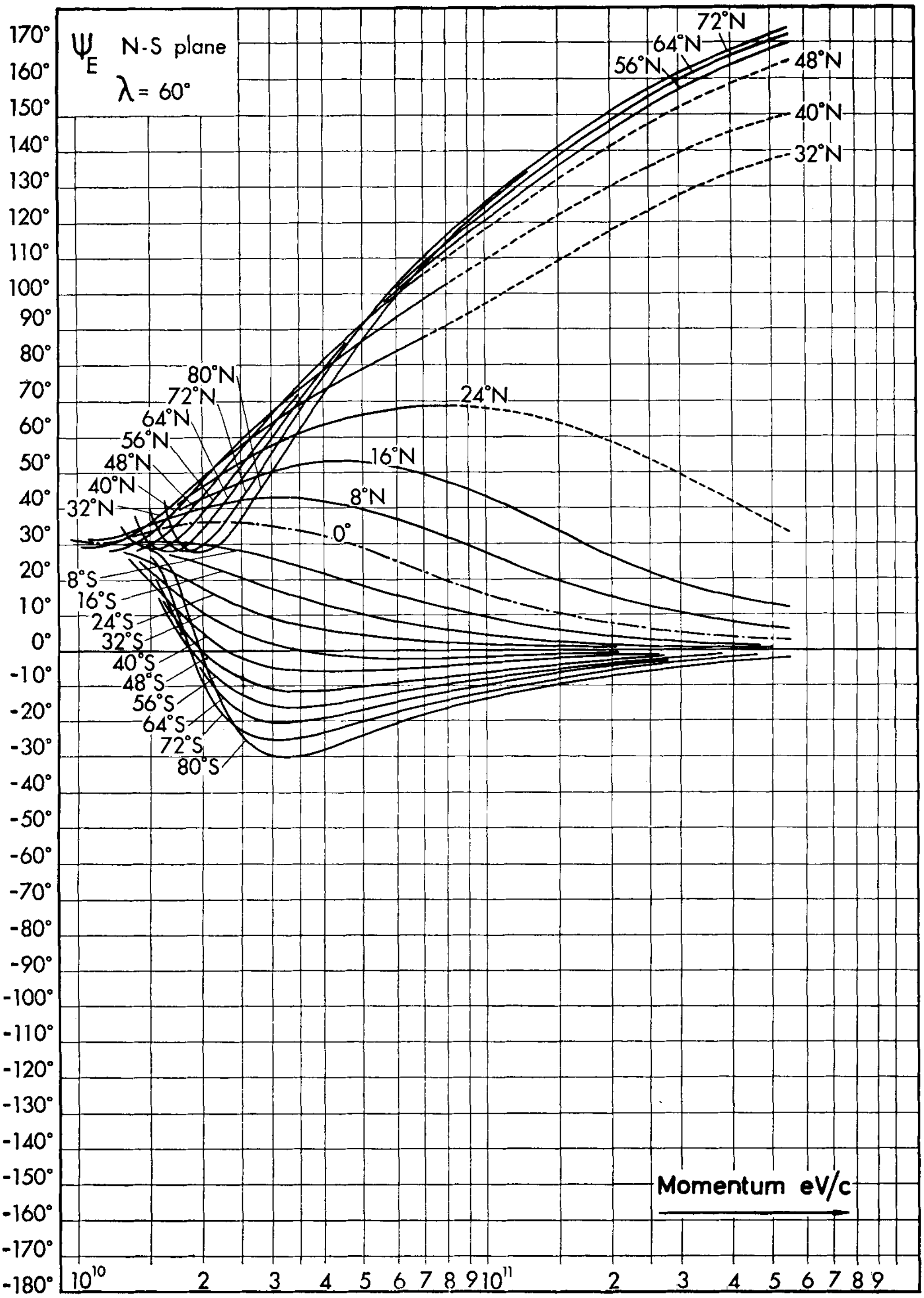

ψ_E N-S plane
$\lambda = 60°$
170°
160°
150°
140°
130°
120°
110°
100°
90°
80°
70°
60°
50°
40°
30°
20°
10°
0°
-10°
-20°
-30°
-40°
-50°
-60°
-70°
-80°
-90°
-100°
-110°
-120°
-130°
-140°
-150°
-160°
-170°
-180°
72°N
64°N
56°N
48°N
40°N
32°N
80°N
72°N
64°N
56°N
48°N
40°N
32°N
24°N
16°N
8°N
0°
8°S
16°S
24°S
32°S
40°S
48°S
56°S
64°S
72°S
80°S
Momentum eV/c
10^{10} 2 3 4 5 6 7 8 9 10^{11} 2 3 4 5 6 7 8 9

Diagram 11.

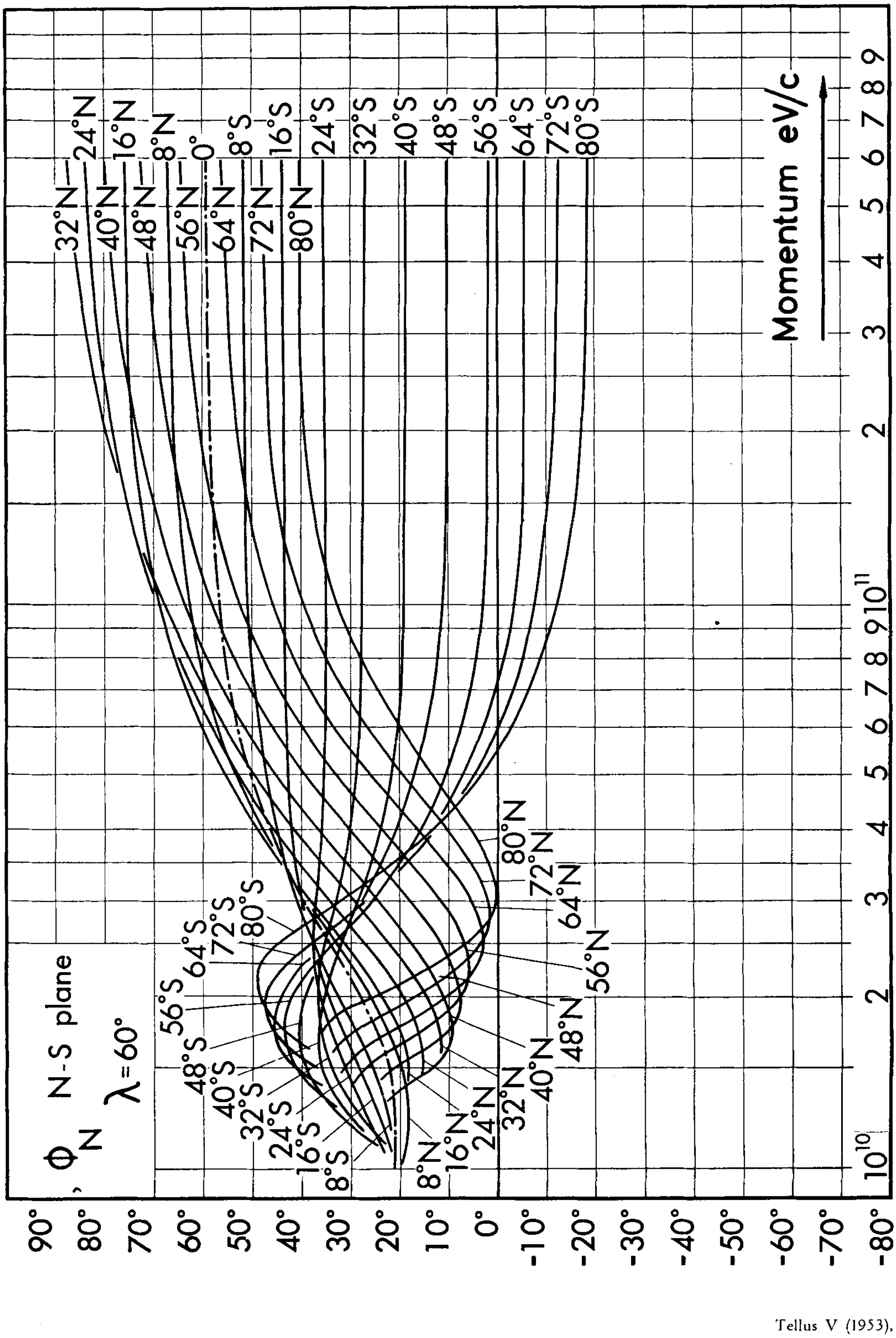
Φ_N
N-S plane
λ=60°
Momentum eV/c
32°N 24°N 40°N 16°N 48°N 8°N 56°N 0° 64°N 8°S 72°N 16°S 80°N 24°S 32°S 40°S 48°S 56°S 64°S 72°S 80°S
80°N 72°N 64°N 56°N 48°N 40°N 32°N 24°N 16°N 8°N
80°S 72°S 64°S 56°S 48°S 40°S 32°S 24°S 16°S 8°S
10^10 2 3 4 5 6 7 8 9 10^11 2 3 4 5 6 7 8 9
90° 80° 70° 60° 50° 40° 30° 20° 10° 0° -10° -20° -30° -40° -50° -60° -70° -80°

Diagram 12.

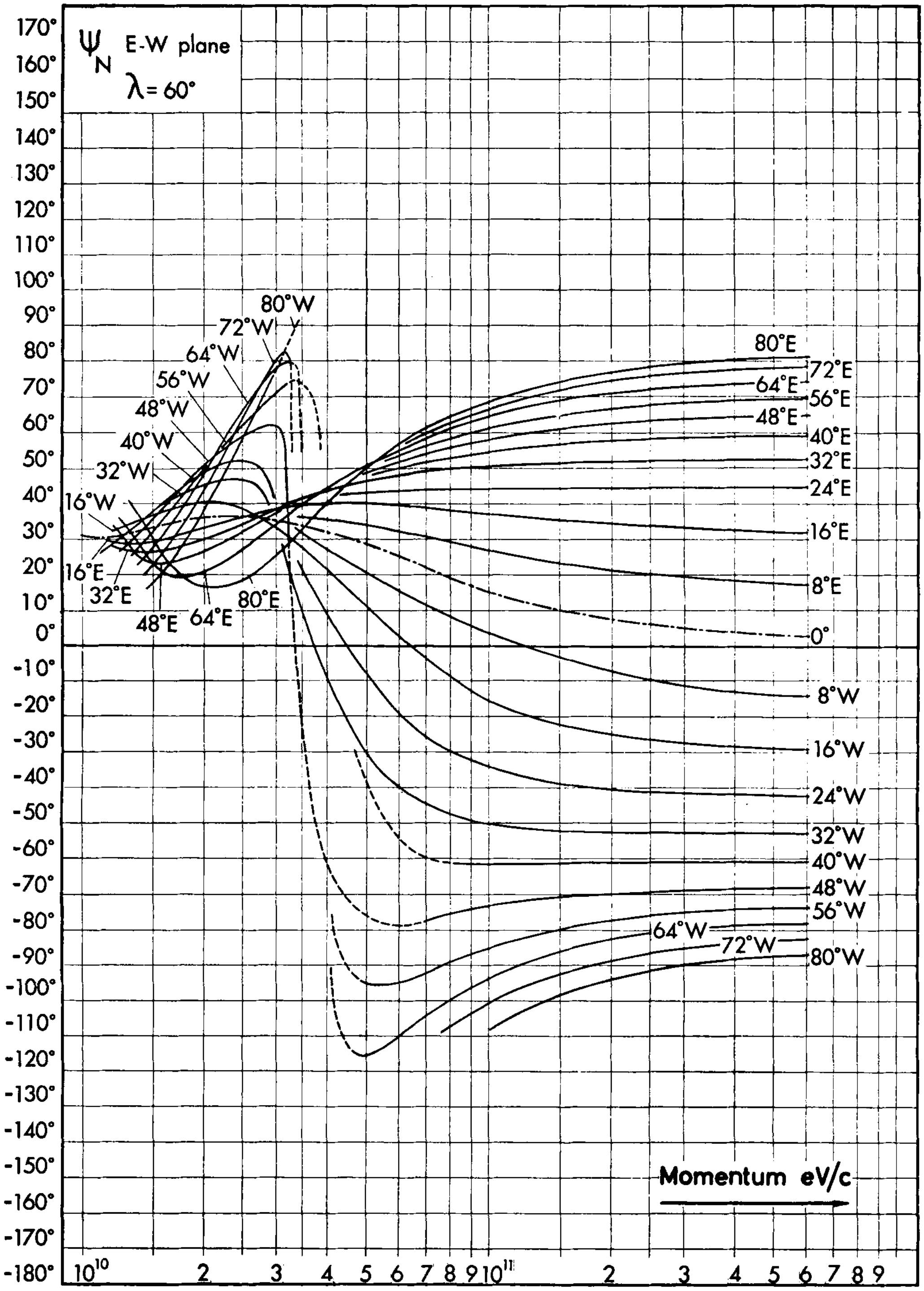

ψ_N E-W plane
$\lambda = 60°$
170°
160°
150°
140°
130°
120°
110°
100°
90°
80°
70°
60°
50°
40°
30°
20°
10°
0°
-10°
-20°
-30°
-40°
-50°
-60°
-70°
-80°
-90°
-100°
-110°
-120°
-130°
-140°
-150°
-160°
-170°
-180°
80°W
72°W
64°W
56°W
48°W
40°W
32°W
16°W
16°E
32°E
48°E
64°E
80°E
80°E
72°E
64°E
56°E
48°E
40°E
32°E
24°E
16°E
8°E
0°
8°W
16°W
24°W
32°W
40°W
48°W
56°W
64°W
72°W
80°W
Momentum eV/c
10^{10} 2 3 4 5 6 7 8 9 10^{11} 2 3 4 5 6 7 8 9

Diagram 13.

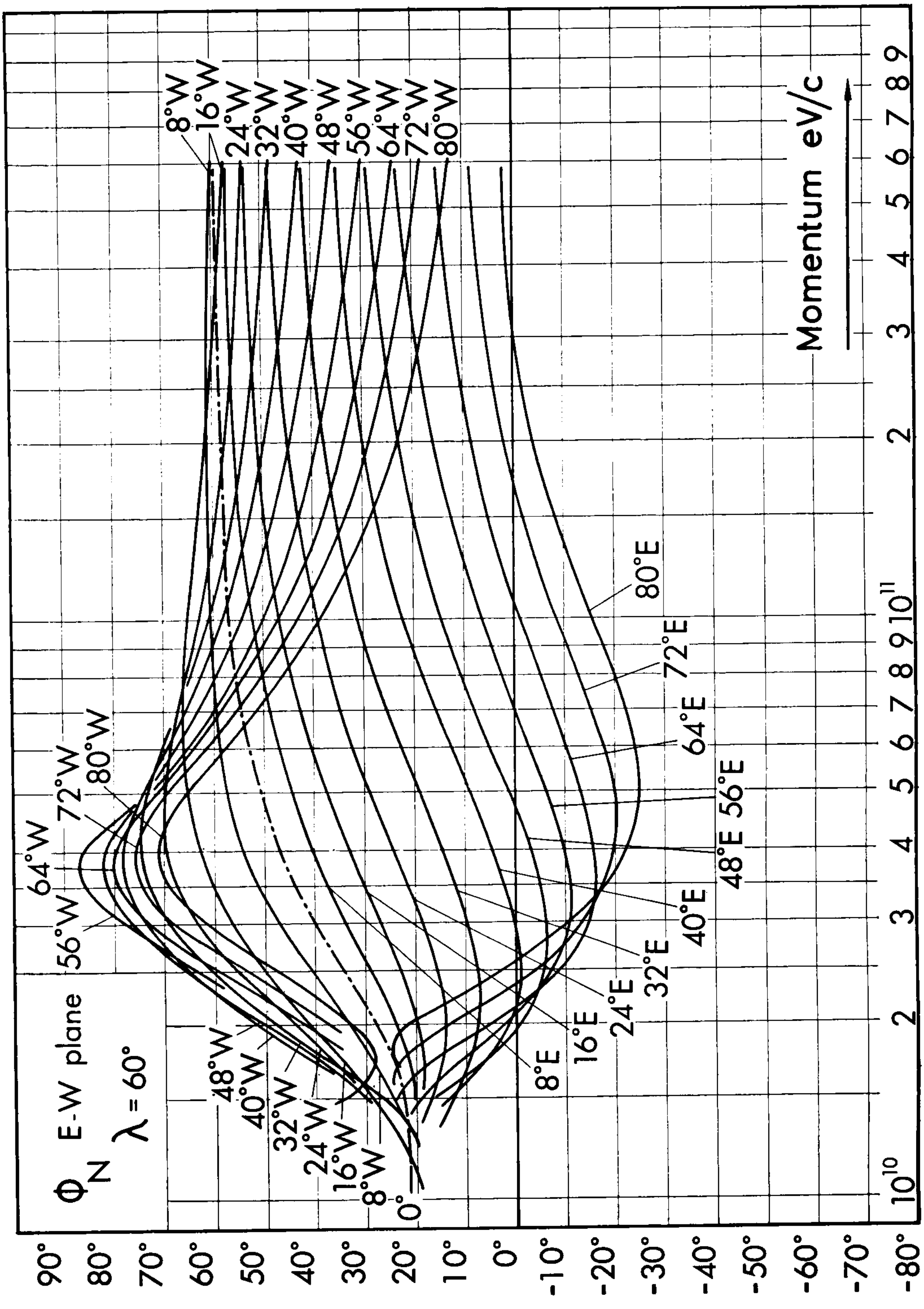

Diagram 14.